Reproductive life history of an acoel worm

Vikram Chandra[#*], Samantha E. Tseng[#], Allison P. Kann, D. Marcela Bolaños, Mansi Srivastava*

Department of Organismic and Evolutionary Biology, Museum of Comparative Zoology, Harvard University, Cambridge, MA 02138

# These authors contributed equally

* Corresponding authors. Emails: vchandra1@fas.harvard.edu, mansi@oeb.harvard.edu

Abstract

Acoel worms belong to an enigmatic and understudied animal lineage (Phylum Xenacoelomorpha). Sparse taxonomic and histological work suggests that these worms exhibit a diversity of reproductive anatomies and likely also a corresponding diversity in reproductive behavior. However, few acoels have been studied in detail. Here, we study the reproductive life history of the three-banded panther worm *Hofstenia miamia*, an acoel that is emerging as a new lab-tractable model system for regenerative biology. Using molecular labeling and histology, we describe *H. miamia*'s reproductive organs, identifying structures previously unknown in acoels. Following a cohort of worms from zygote to adulthood, we quantify the developmental dynamics of their reproductive organs, and find that these organs are assembled step-wise, at increasing body sizes. Studying the dynamics of organ growth during regeneration and de-growth in starving adult worms, we show that reproductive organs follow similar growth rules in these contexts, suggesting that their development and maintenance is regulated by a size-dependent program. Finally, we study egg-laying behavior, finding that *H. miamia* lay their eggs through

their mouths after loading them into their pharynges. Experimentally varying the worms' environment reveals that the worms make active decisions about when and where to lay their eggs. In summary, our work establishes foundational knowledge to enable the experimental study of reproductive anatomy, physiology, and behavior in acoels.

Introduction

Reproduction is critical for evolutionary success, and animals display great diversity in their reproductive life histories. The structures and strategies employed for reproduction have been relatively well-studied in some animal lineages, such as arthropods and vertebrates (1). However, the complexities of reproductive biology in many animal phyla remain poorly studied. For example, Phylum Xenacoelomorpha, which includes acoels, nemertodermatids, and xenoturbellids, represents a deep-diverging lineage of animals with bilateral symmetry (2–4) (Fig. 1A). Whereas reproductive structures have been reported in a handful of species in this phylum of largely marine worms, many aspects of reproduction such as sexual maturation, aging, mating, and egg laying are unexplored (Fig. 1B). Here, we apply a diverse toolkit for a systematic study of reproductive biology in the acoel *Hofstenia miamia*, which has emerged as a new laboratory research organism.

There are roughly 400 described species of acoel worms (5–7). Traditionally, acoel taxonomy is done through the description and analysis of morphological characters observable in histology slice preparations of specimens collected from the field (8). A few exceptions notwithstanding, these data also constitute the majority of what we know about reproduction in acoels. Acoels are thought to be simultaneous hermaphrodites (with few exceptions (9, 10)); once mature, each worm has both male and female reproductive structures (8). Unlike many other aquatic animals, e.g., cnidarians, poriferans, echinoderms, that reproduce sexually through spawning and external fertilization (11), acoels have been reported to reproduce

53 sexually through internal fertilization (6). Acoel worms exhibit a large diversity in their
54 reproductive anatomy (Fig. 1B, Table S1). This anatomical variation likely predicts variation in
55 reproductive physiology and behavior, but little is known about how most acoels develop their
56 reproductive organs, mate, or lay eggs. For instance, species lacking a female gonopore and a
57 seminal bursa (a sperm storage organ) likely mate through competitive hypodermic
58 insemination, but mating behavior has not been observed in the majority of these species. The
59 lack of a female gonopore in these species predicts that eggs must be laid either through
60 rupture of the body wall (12–14) or through the mouth, but few species have been observed
61 laying eggs at all, and despite speculation, no animal has ever been shown to lay eggs through
62 its mouth.

63 The majority of observations of reproductive behavior in acoels are based on a small
64 handful of species within one family (the Convolutidae) that has several derived traits (8).
65 Historically, it has been challenging to study acoel reproduction in controlled conditions because
66 few acoels have been cultured in the lab (12, 15–17), and most descriptions of acoel
67 reproduction occurred at a time when modern imaging methods did not exist or were
68 inaccessible. To improve our understanding of acoel life histories, we studied reproduction in an
69 early-diverging acoel, the three-banded panther worm *Hofstenia miamia* (Fig. 1C). *H. miamia* is
70 an emerging model system with several features that allow us to study it in controlled
71 conditions: *H. miamia*'s life cycle can be closed in the lab (rearing worms from embryo to gravid
72 adult takes 2-3 months), and a growing array of experimental tools is available to observe and
73 manipulate the worm (18–23).

74 *H. miamia* is a member of the family Hofsteniidae, which contains three genera (5, 24)
75 and is placed as an early-diverging lineage among acoels (8). Five species have been
76 described within the genus *Hofstenia*. Histology-based work has described the coarse anatomy
77 of reproductive organs in *Hofstenia* (24–28). However, the fine structure of these organs, how
78 they grow and develop, and how they function in the course of reproductive behavior remains

unknown. Here, to understand the reproductive life history of *H. miamia*, we use a combination of light and confocal microscopy, fluorescence in situ hybridization, immunofluorescence, and histology, as well as observations of reproductive development and behavior in controlled conditions. We describe the fine structure of *H. miamia*'s reproductive organs, its developmental and regenerative trajectory, and how this worm lays eggs. These findings establish a foundation for the mechanistic study of reproduction in an acoel worm.

Results

An overview of *Hofstenia miamia*'s reproductive anatomy

The genus *Hofstenia* was first described by Bock (25) and based on studies of the three currently-recognized species, *H. atroviridis*, *H. miamia*, and *H. arabiensis*, *Hofstenia* are considered to be simultaneous hermaphrodites (24–28). The three species are also described as having an anterior male reproductive system including a seminal vesicle, prostatic vesicle, a penis with sclerotized needles, diffuse ventrolateral testes, and a male gonopore near the mouth (24–28). The female reproductive system, as described, includes two ovaries spanning the posterior two-thirds of the worm. *Hofstenia miamia* is likely the most common and widespread species within the genus, with a geographic distribution including the North Atlantic, the Caribbean, the Bahamas, and the Florida coast (24–28). Although multiple authors have described elements of *H. miamia*'s reproductive systems, these descriptions were all based on worms roughly 5-8mm in length (24–28). In our lab cultures of *H. miamia*, fully grown adult worms can be over 1.4cm in length, and we reasoned that their anatomy could be subtly different. We therefore began by re-examining the coarse anatomy of *Hofstenia miamia*.

We anesthetized adult worms, mounted them ventral side up on a slide, and imaged them through a dissecting microscope to reveal coarse reproductive organization. As expected, we found that *H. miamia*'s male copulatory structures are located in the anterior of the animal, just posterior to the mouth (Fig. 1D,E). These male structures are located within a translucent tube-like region, located close to the ventral surface of the worm, immediately ventral to the pharynx. We observed two white opaque regions within the male copulatory apparatus, located towards its posterior (Fig. S1A). The larger, posterior oval structure corresponds to the seminal vesicle, while the smaller, teardrop-shaped anterior structure corresponds to the prostatic vesicle (Fig. 1D,E; Fig. S1A), traditionally referred to as the vesicula granulorum (24–28). Previous work reported that *H. miamia* has a penis or stylet: a sperm-delivery organ containing rigid needles. This structure is typically difficult to see in these imaging conditions. However, we identified a small aperture immediately posterior and ventral to the mouth (Fig. S1A), and we observed that the worm extended its penis through it, suggesting that this aperture is the male gonopore, and confirming the location of the penis in the anterior of the worm.

As previously described (24–28), we found that the female reproductive system occupies the posterior two-thirds of the worm. This system appears relatively simple, with numerous eggs grouped into three distinct clusters (Fig. S1B). One lateral group on each side of the body, near the margins, extends along the anterior-posterior axis. These lateral clusters contain oocytes of various sizes, likely corresponding to different stages of maturation, each with a visible nucleus, and have been identified as the ovaries in historical reports (24–28). There is no obvious organization of oocytes in the ovaries along the anterior-posterior, dorso-ventral, or medio-lateral axes.

Posterior to the pharynx, there is often a cluster of spherical eggs (Fig. 1D,E; Fig. S1C). The number of eggs at this position is highly variable, ranging from zero to over a dozen eggs. In *H. atroviridis*, Bock (25) speculated that these eggs are mature, fertilized, and ready to be laid. This is consistent with our observations: these eggs appeared uniformly sized and lacked a

129 visible nucleus, in contrast to the oocytes in the ovaries, suggesting that eggs in this area may
130 already be fertilized. To test whether these eggs were indeed zygotes, we dissected out eggs
131 from this central cluster, as well as from the ovaries. We found that 46/56 eggs removed from
132 the central cluster developed and hatched into juvenile worms, in line with previously
133 established embryonic trajectories (Fig. S1D) (23). Meanwhile, all eggs dissected from the
134 ovaries disintegrated within 48 hours. The eggs in this central cluster are therefore mature, likely
135 fertilized, and ready for laying while eggs in the ovaries are immature or unfertilized. Overall,
136 these observations confirm and extend previous descriptions of *H. miamia*, and provide a high-
137 level overview of *H. miamia*'s reproductive anatomy. Next, we sought to apply a variety of
138 experimental approaches to obtain a detailed understanding of these structures and their
139 development.
140

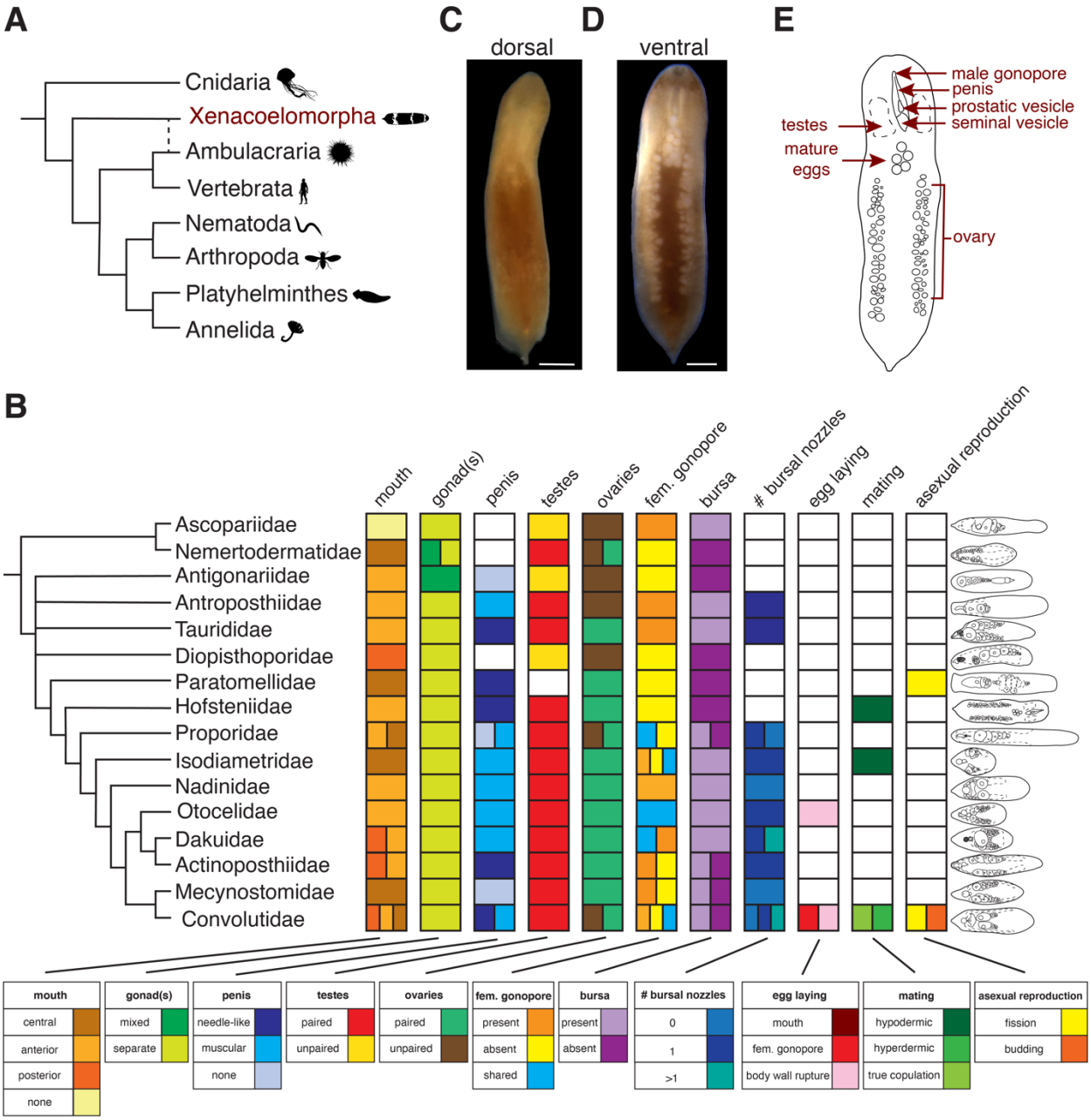

Figure 1: *Hofstenia miamia* is a model acoel worm for studying Xenacoelomorph life history. (**A**) Xenacoelomorpha is a deep-diverging bilaterian lineage of aquatic worms. Phylogeny modified from (18). Animal icons are from phylopic.org, and are in the public domain. (**B**) Family-level phylogeny of Acoelomorpha (Nemertodermatida, Acoela) showing anatomical and reproductive life history traits (Table S1): position of the mouth, whether gonads are mixed or separated by sex, penis type, paired or unpaired testes, paired or unpaired ovaries, ovary organization, presence or absence of a female gonopore, presence or absence of a seminal bursa, the number of associated bursal nozzles, egg-laying mode,

149 mode of sexual reproduction, and mode of asexual reproduction (see Table S2 for definitions of terms
150 and categories). Schematic for each family shows reproductive anatomy of a representative species
151 (Table S1). White boxes represent unknown phenotypic states, and in the case of asexual reproduction,
152 its possible absence. Phenotypic classifications are from (10, 12–15, 24, 25, 27–51) (**C**) Dorsal view of
153 *Hofstenia miamia*. (**D**) Ventral view of an adult *Hofstenia miamia*; most reproductive structures are visible
154 in this view. (**E**) Schematized view of the ventral surface of a worm with known reproductive structures
155 illustrated. Scale bars: 1 mm (C, D).
156

157 **Development of reproductive organs**

158 How reproductive structures develop as animals reach sexual maturity is not well understood in
159 any xenacoelomorph species. In *H. miamia*, juvenile worms that hatch from eggs have no
160 reproductive structures, and previous observations suggested that these develop over a month
161 later as the worms grow toward adulthood (18, 23). Our initial observations (Fig. 1D) showed
162 that we could identify major reproductive structures in a non-invasive manner, simply by imaging
163 the ventral surfaces of anesthetized worms using a stereo microscope. Using this method in
164 combination with our ability to study all stages of the life cycle in *H. miamia*, we sought to
165 determine the timeline and dynamics of reproductive development. We reared 42 zygotes in
166 isolation and monitored their growth through development (Fig. 2A), precisely controlling their
167 rearing environment such that each animal had access to a standardized amount of seawater
168 and a defined amount of food (see Methods). To determine how nutrition affects reproductive
169 development, we split the cohort of zygotes into two groups that were fed differently. For each
170 group, we gradually increased the amount of food they were given as they grew larger, to
171 ensure that worms had enough food to minimize developmental time. These food increases
172 occurred periodically, but were delayed by two weeks for one feeding group (Fig. S2A). Twice
173 weekly, we captured images of the ventral surface of each worm and quantified the size of each
174 visible reproductive structure. Two embryos did not hatch, and two worms died during the

175 course of the experiment (likely due to handling error). Four worms were removed from the
176 experiment at different timepoints for additional imaging, resulting in 34 worms that we followed
177 into adulthood (Fig. S2B).

178 We found that worms maintained their aspect ratio from hatchling to adult, growing
179 proportionally over time (Fig. 2A-D; Fig. S2C). At every stage of development, the size of each
180 reproductive organ scaled with body size once that organ appeared (Fig. 2E-G). Worms with
181 delayed increases in feeding displayed corresponding delays in their growth, both in their body
182 size (Fig. S2D) and in the timing of appearance of their ovary and seminal vesicle (Fig. 2H,I).
183 Worms with delayed feeding developed a penis and a seminal vesicle at a slightly smaller body
184 size, but did not significantly differ in the body size at which their ovaries first appeared. Overall,
185 these data suggest that the growth and differentiation of reproductive structures is generally
186 coupled to the worm's body size.

187 For both treatments, we found that reproductive development generally occurs in a
188 stepwise fashion. Newly hatched animals possess all major somatic organs (such as a brain,
189 muscle system, pharynx, gut, etc. (21, 23)), but lack all reproductive structures (Fig. 2A,B). 4-6
190 weeks after being laid, when the worm is about 3.02 ± 0.6 mm (mean ± SD) in length, the
191 anterior-ventral tissue housing the future male copulatory apparatus becomes visibly less
192 dense, and a groove becomes apparent in the ventral surface. Soon after, the male gonopore
193 becomes detectable posterior to the mouth. Sperm begin to accumulate in the seminal vesicle
194 around 35 days post laying (dpl), once a worm is about 4.41 ± 0.9 mm (mean ± SD) long.
195 Shortly after, when a worm is 5.6 ± 0.9 mm (mean ± SD), the first oocytes become visible in
196 nascent ovaries. These ovaries grow with the worm over time, with existing oocytes maturing
197 and new ones continuously added. Around two months after being laid, typically after a worm is
198 8.73 ± 1.2 mm in length, eggs appear near the base of the pharynx (Fig. 2A,B,H,I). These eggs
199 are laid within hours or days, and they develop and hatch into juvenile worms. Given that these

worms were isolated since birth, this suggests that *H. miamia* can reproduce through both mating and self-fertilization.

To visualize the extent to which reproductive structures develop in a sequence, we ranked each structure in each worm by its date of appearance (Fig. 2J). All worms, without exception, first developed a penis. A few worms simultaneously developed a seminal vesicle; in most other worms, this structure appeared second, with a few developing their seminal vesicle concurrent with nascent ovaries. Ovaries always appeared before the first fertilized eggs are seen in the central region. Next, we asked whether the left and right ovaries of each worm developed in synchrony. We found that on the first day that an ovary was visible, 34/34 worms had both ovaries visible. Partial regression analysis revealed that the sizes of the two ovaries within a worm are strongly correlated, even when correcting for body size (Fig. S2E). This suggests that an active developmental process synchronizes the ovaries within individual worms. Taken together, these observations suggest that the development of reproductive organs is strongly coupled to body size.

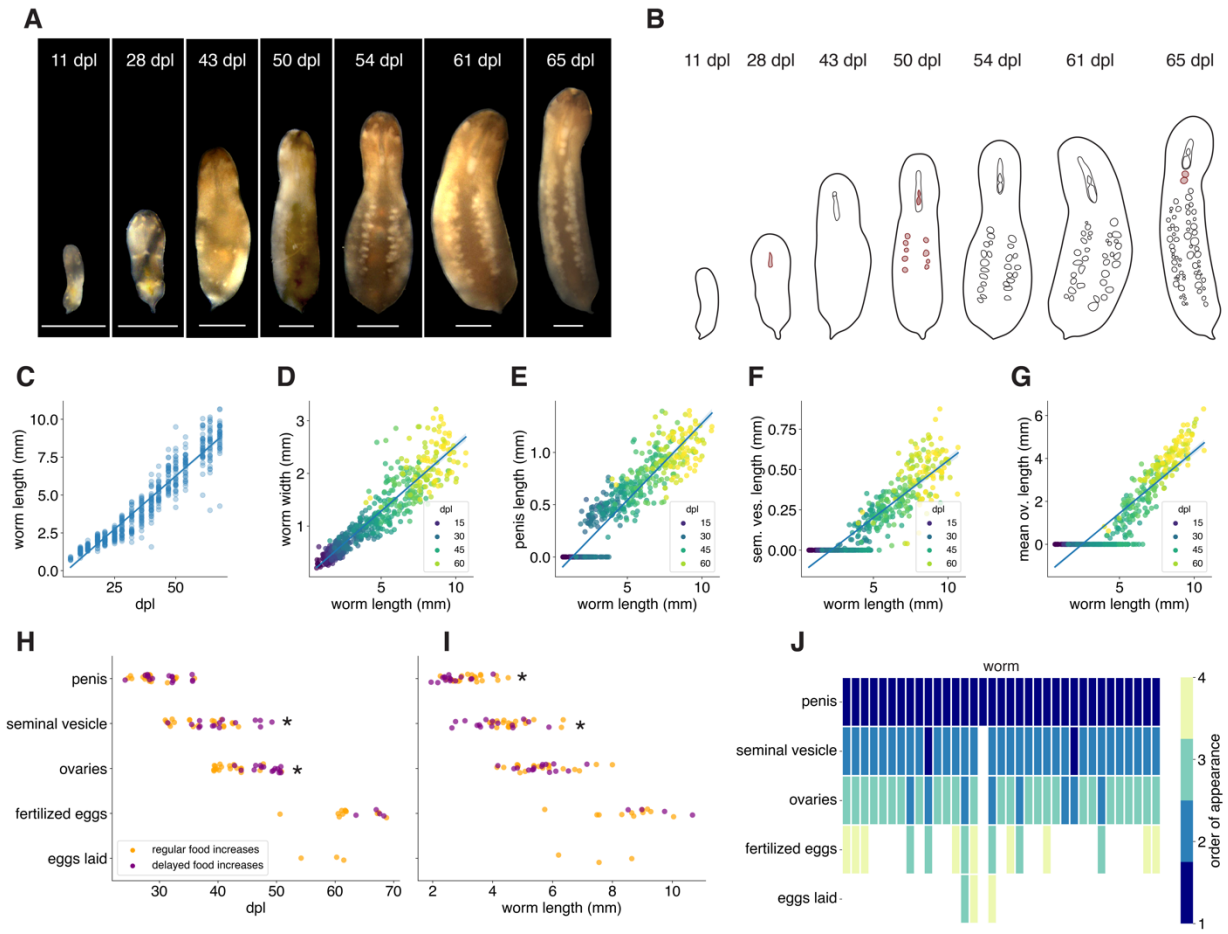

Figure 2: Reproductive organs develop stepwise following scaling rules. (**A**) Time course of one worm through developmental time from hatchling to reproductively mature adult. (**B**) Schematic of timecourse shown in (**A**) with key reproductive developments illustrated. (**C**) The length of worms increases over time ($R^2 = 0.91$, $p < 0.001$), and worms grow proportionally: their length scales with their width ($R^2 = 0.85$, $p < 0.0001$) (**D**).The length of each reproductive organ scales with increases in body size (penis: $R^2 = 0.85$, $p < 0.0001$; seminal vesicle: $R^2 = 0.82$, $p < 0.0001$; ovaries: $R^2 = 0.82$, $p < 0.0001$) (**E-G**). Comparing the date of first appearance of reproductive organs between worms fed differently reveals that these organs develop as a function of body size, but not age. (**H**) Worms with delayed feeding increases had significant delays in the appearance of their seminal vesicle and ovaries, but not the penis (Welch's t test for date of appearance for penis: $p = 0.08$, seminal vesicle: $p = 0.04$, ovary: $p <$ 10^-6; $n \geq 15$). (**I**) Worms with delayed feeding increases had a smaller body length when a penis and

227 seminal vesicle appeared, but not when ovaries appeared (Welch's t test for length on date of
228 appearance for penis: $p = 0.005$, seminal vesicle: $p = 0.03$, ovary: $p = 0.74$; $n \geq 15$). Asterisks indicate
229 statistical significance. (**J**) Ranking the order in which reproductive organs appear (y-axis) in developing
230 worms reveals a stepwise pattern of reproductive differentiation. The x-axis shows individual worms. dpl =
231 days post laying. Scale bars: 1 mm.
232

233 **De-growth and regeneration of reproductive organs**

234 Next, we asked whether these patterns of growth persisted in different contexts. Anecdotal
235 observations suggested *H. miamia* tolerates long periods of starvation but gradually shrinks in
236 size when deprived of food. We starved a cohort of adult worms and quantified the de-growth of
237 their reproductive organs over time (Fig. 3A,B). We found that all worms survived over three
238 months of continuous starvation, gradually shrinking over time (Fig. 3C). Worms maintained
239 their aspect ratios as they shrank (Fig. 3A,B,D), and their reproductive organs shrank
240 correspondingly (Fig. S3A-E). Partial regression analysis of shrinking ovaries showed that they
241 shrink synchronously (Fig. S3F), suggesting active coordination of de-growth.

242 We also asked how reproductive organs change in another growth context. *H. miamia*,
243 like many acoels, is an excellent regenerator, and can regenerate all tissues from a wide range
244 of initial tissue configurations (18, 52). We amputated and followed adult worms in three ways:
245 by separating the tip of the tail (which contained no reproductive structures) and studying how
246 they regenerated the majority of their organs, by cutting worms sagittally and studying how they
247 regenerated their missing half, and by separating heads from tails and studying how these head
248 fragments regenerated their tails and the posterior region of their ovaries (Fig. 3E). Head and
249 tail fragments both gradually increased in size, with tail fragments growing much faster (Fig.
250 S3G-M). Within two weeks, most of these fragments had regained the characteristic shape of
251 intact homeostatic worms, and were foraging apparently normally. Sagittally-cut fragments first

shrank in size before subsequently growing (Fig. S3M), and appeared to take longer to fully regain normal worm-like appearance (Fig. S3I,J). All reproductive organs gradually regenerate, with growth dynamics contingent on the nature of the injury (Fig. 3F-N; Fig. S3G-L,N,O).

The scaling relationships we found between reproductive organs and body size during post-embryonic development and juvenile growth generalized to both de-growth and regeneration (Fig. 3O-Q). We then studied the smallest body size at which starving worms retained their organs, as well as the body size at which reproductive organs first appeared in regenerating fragments, comparing them to the sizes at which these organs first appear during the normal developmental transition from juvenile to adult (Fig. 3R). In general, starving worms lost reproductive organs in the opposite order to which they gained them, first losing fertilized eggs, then ovaries, and eventually losing their seminal vesicle (Fig. 3S). However, after three months of starvation, most worms continued to retain their penes despite being below the threshold size at which we would expect to see loss of this organ (Fig. 3R). In regenerating tail fragments, the male reproductive structures generally developed before the female reproductive structures, following similar stepwise patterns to developing juvenile worms (Fig. 3T).

In regenerating head fragments and in sagittally-cut worms, each worm fragment retained one of its two ovaries immediately after amputation. These ovaries first partially degenerated before growing back (Fig. 3J), suggesting that there is active destruction of tissue during the early stages of regeneration. This is consistent with the loss of germline marker expression during early regeneration (19). The missing ovary began to grow back roughly one month after amputation. We found that the ovaries grew asymmetrically in these worms, with the new ovary growing faster (Fig. 3J). This suggests the existence of an active growth mechanism to ensure that both ovaries reach a symmetric target size.

Together, our results suggest the existence of a size-dependent differentiation program that regulates the development of reproductive organs, as well as active tissue growth and destruction mechanisms to ensure organ symmetry. It is likely that these processes regulate

278 reproductive organ growth in a variety of different developmental contexts, including the
279 transition from juvenile to adult worm, regeneration after injury and tissue loss, and during
280 starvation-induced de-growth.
281

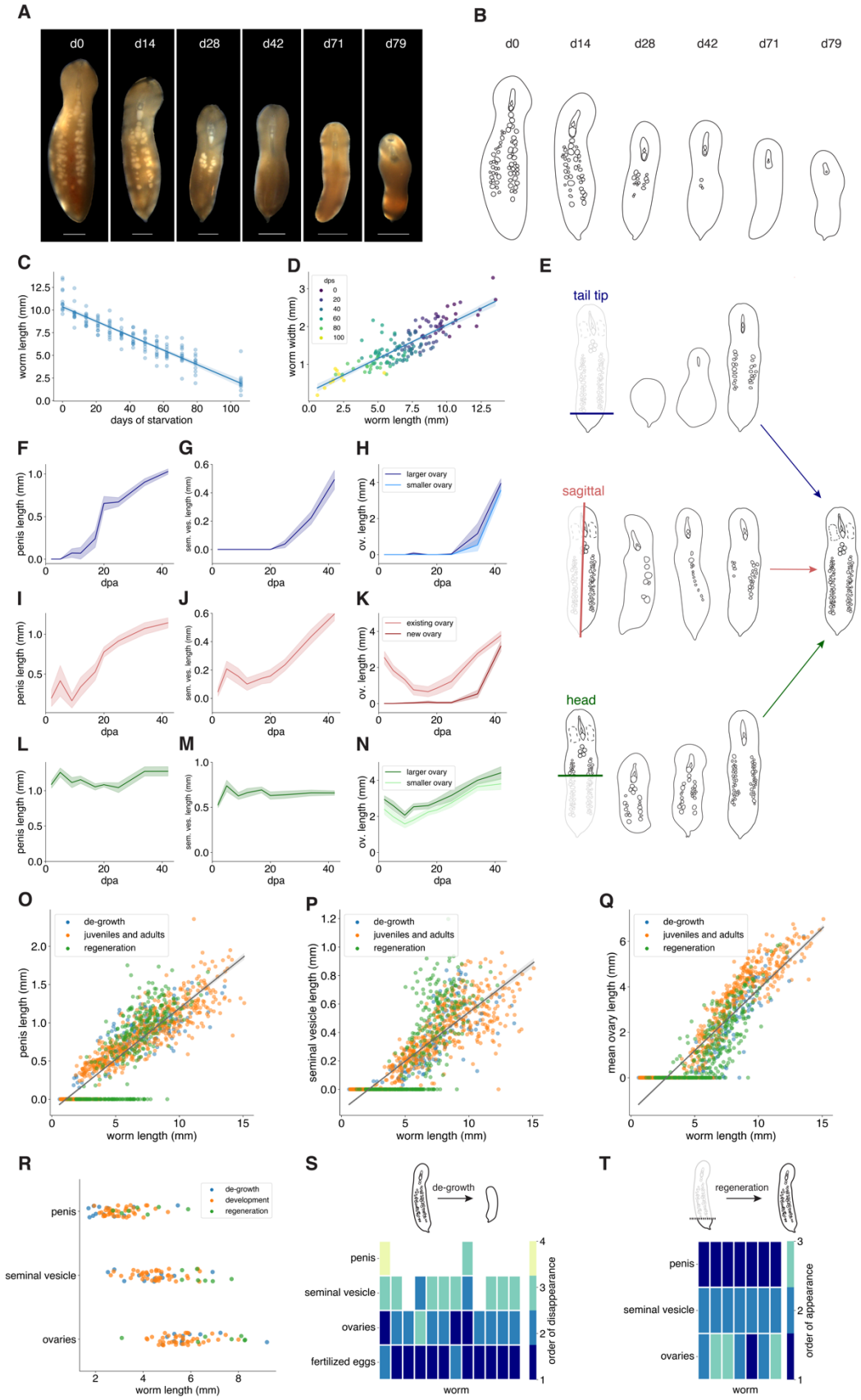
A
d0
d14
d28
d42
d71
d79
B
d0
d14
d28
d42
d71
d79
C
worm length (mm)
days of starvation
D
dps
0
20
40
60
80
100
worm width (mm)
worm length (mm)
E
tail tip
sagittal
head
F
penis length (mm)
dpa
G
sem. ves. length (mm)
dpa
H
larger ovary
smaller ovary
ov. length (mm)
dpa
I
penis length (mm)
dpa
J
sem. ves. length (mm)
dpa
K
existing ovary
new ovary
ov. length (mm)
dpa
L
penis length (mm)
dpa
M
sem. ves. length (mm)
dpa
N
larger ovary
smaller ovary
ov. length (mm)
dpa
O
de-growth
juveniles and adults
regeneration
penis length (mm)
worm length (mm)
P
de-growth
juveniles and adults
regeneration
seminal vesicle length (mm)
worm length (mm)
Q
de-growth
juveniles and adults
regeneration
mean ovary length (mm)
worm length (mm)
R
de-growth
development
regeneration
penis
seminal vesicle
ovaries
worm length (mm)
S
de-growth
penis
seminal vesicle
ovaries
fertilized eggs
order of disappearance
worm
T
regeneration
penis
seminal vesicle
ovaries
order of appearance
worm

Figure 3: Reproductive organ development follows similar rules in different growth contexts. (**A**) Time course of a starving worm undergoing de-growth and step-wise loss of reproductive organs. (**B**) Schematic of reproductive organ degradation over the course of starvation-induced de-growth. (**C**) Worm length decreases over the course of degrowth ($R^2 = 0.85$, $p < 0.0001$). (**D**) Worms shrink as they grow; their lengths and widths decrease proportionally ($R^2 = 0.73$, $p < 0.0001$). dps = days post onset of starvation. (**E**) Schematic of regeneration of the penis, seminal vesicle, and ovaries following three different amputations. (**F-N**) Growth dynamics of reproductive organs (within column) for each of three amputations (within row). (**O-Q**) The size of reproductive structures scale according to patterns conserved across development, de-growth, and regeneration (penis: $R^2 = 0.75$, $p < 0.0001$; seminal vesicle: $R^2 = 0.68$, $p < 0.0001$; ovary: $R^2 = 0.8$, $p < 0.0001$). (**R**) Across different growth contexts, reproductive organs appear or disappear at roughly consistent body lengths. Ranking the order in which reproductive structures are lost in worms undergoing de-growth (**S**) and regenerating worms (**T**) shows that organs are gained and lost in roughly the same order in all growth contexts. The x-axis shows individual worms in these plots. dpa = days post amputation. Scale bars: 1 mm.

The male reproductive system

The results above show that imaging using a stereo microscope, even at low resolution, provides a wealth of information about reproductive morphology and development. However, the detailed morphology of these structures cannot be ascertained based on these images. We therefore used a combination of histology, immunofluorescence, staining with live dyes, and fluorescence *in situ* hybridization (FISH) to visualize male reproductive structures at high resolution in worms at different stages of development (Fig. 4A; Fig. S4A,B; S5A).

The most anterior part of the male copulatory apparatus is the penis. This structure is difficult to visualize under conventional illumination, but can be seen when worms extend it, which we have observed them do both spontaneously and during mating (data not shown). Staining fixed worms with the dye SiR-actin labels the structure clearly, and in early adult worms

310 lacking ovaries, we were able to use confocal imaging to visualize it at high resolution (Fig. 4B-
311 C). Components of the penis can also be seen clearly in histological sections of adult worms
312 (Fig. 4D). These show that the penis consists of a bundle of rigid needle-like structures (referred
313 to as stylet needles) (Fig. 4E-G). Our observations of the stylet match the description of the
314 cuticular rods described in other species in the genus and in other studies of *Hofstenia miamia*
315 (24–28). The stylet is situated immediately posterior to the base of the penis sheath - a long,
316 conical structure (Fig. 4C,D; Fig. S4E,H,J; Video 1). The base of the sheath is cup-shaped, and
317 is lined by posterior-facing hair-like extensions (Fig. 4G). At its anterior end, it connects to the
318 male gonopore (Fig. 4C, Fig. S5B), both of which are lined with cilia (Video 1,2), consistent with
319 reports of a ciliated sheath in other hofsteniid species (24–28). Immunofluorescence with an
320 antibody against Par3 (see Methods) revealed a set of cells that resemble neurons encircling
321 the base of the sheath (Fig. S4C,D). Further studies will be needed to establish the true identity
322 and function of these cells.

323 Next, we focused on the teardrop-shaped prostatic vesicle, which is situated anterior to
324 the seminal vesicle and is connected to the posterior end of the penis stylet (Fig. 4H-I). Our
325 histological studies shows that the prostatic vesicle is surrounded by glands that likely produce
326 granular secretions (Fig. S5,H). The secretions of this organ mix with the sperm as it passes
327 through, and it has been speculated that it is important for the health and vitality of the sperm,
328 although the nature of this secretion has not been identified (53, 54). Unexpectedly, our
329 immunofluorescence experiments revealed a thin layer of cells enclosing the prostatic vesicle
330 (Fig. 4I). This layer may be an epithelial tissue most likely associated with the extravesicular
331 prostatic glands. The interior of the prostatic vesicle contains densely-packed sperm cells (Fig.
332 4D,I; Fig. S4E; Fig. S5C-E; Fig. S5F-G).

333 The posterior of the male copulatory apparatus contains the seminal vesicle (Fig. 4J).
334 Histology, as well as nuclear staining of this organ in adult worms (Fig. 4K-L; Fig. S5C-E,G,H)
335 reveals that it consists entirely of sperm cells. To confirm this, we dissected the seminal vesicle

336 out of adult worms, and stained it with a nuclear dye – we found that individual cells emerged
337 from the structure over time, and high-magnification imaging showed that they were indeed
338 sperm cells, each with a long (~23um) nucleus, and a 22um-long flagellum (Fig. 4M). During
339 one mating event, we observed a failed attempt at insemination by a worm that resulted in the
340 release of a packet of sperm outside its partner. We recovered this 0.6 mm-long packet of
341 sperm (Fig. S4F-G) and found that it consisted of cells with the same morphology as those in
342 the seminal vesicle (Fig. S4H), confirming that these are indeed sperm. Histological staining as
343 well as immunofluorescence staining against the muscle marker tropomyosin, showed that the
344 seminal vesicle and prostatic vesicle are both encircled by layers of muscle (Fig. S4E; Fig. S5C-
345 H).

346 We then turned to the testes (Fig. 4N). Nuclear staining of adult worms (cut sagittally
347 prior to fixation) revealed dense bundles of sperm in the parenchyma, extending much of the
348 way around the circumference of the worm (Fig. O-Q). The location of the testes is consistent
349 with previous descriptions (24–28). Our histology of transverse sections of adult worms
350 confirmed these observations (Fig. 4R-T). Immunofluorescence staining against tropomyosin
351 showed that the testes are embedded within muscle layers in the parenchyma (Fig. S4L). To
352 understand the structure of the testes better, we used FISH for putative germline markers
353 revealed by our previous single-cell RNA-sequencing data (19). We found that one of these
354 marker genes, *pa1b3-2*, specifically labeled the testes (Fig. 4U), showing them to be paired,
355 lateralized structures in the worm's anterior.

356 Finally, we conducted a developmental time course study to visualize the maturation of
357 the male reproductive system. In juvenile worms, at early developmental stages, actin staining
358 reveals the prostatic vesicle is virtually absent and progressively emerges as the animal
359 matures (Fig. S4A). These data also show that the sheath grows progressively. We also
360 performed FISH to detect mRNA for *pa1b3-2*, using worms across multiple developmental
361 stages. In juvenile worms (smaller and lacking mature reproductive structures), there was no

362 expression (Fig. S4I-K). In older worms we began to see expression of *pa1b3-2*, with the
363 expression domain expanding along the anterior-posterior axis with age (Fig. S4I-K).
364 Together, our data provide a high-resolution view of *H. miamia's* elaborate male
365 reproductive morphology, and allow a more comprehensive understanding of its organization
366 and function.
367

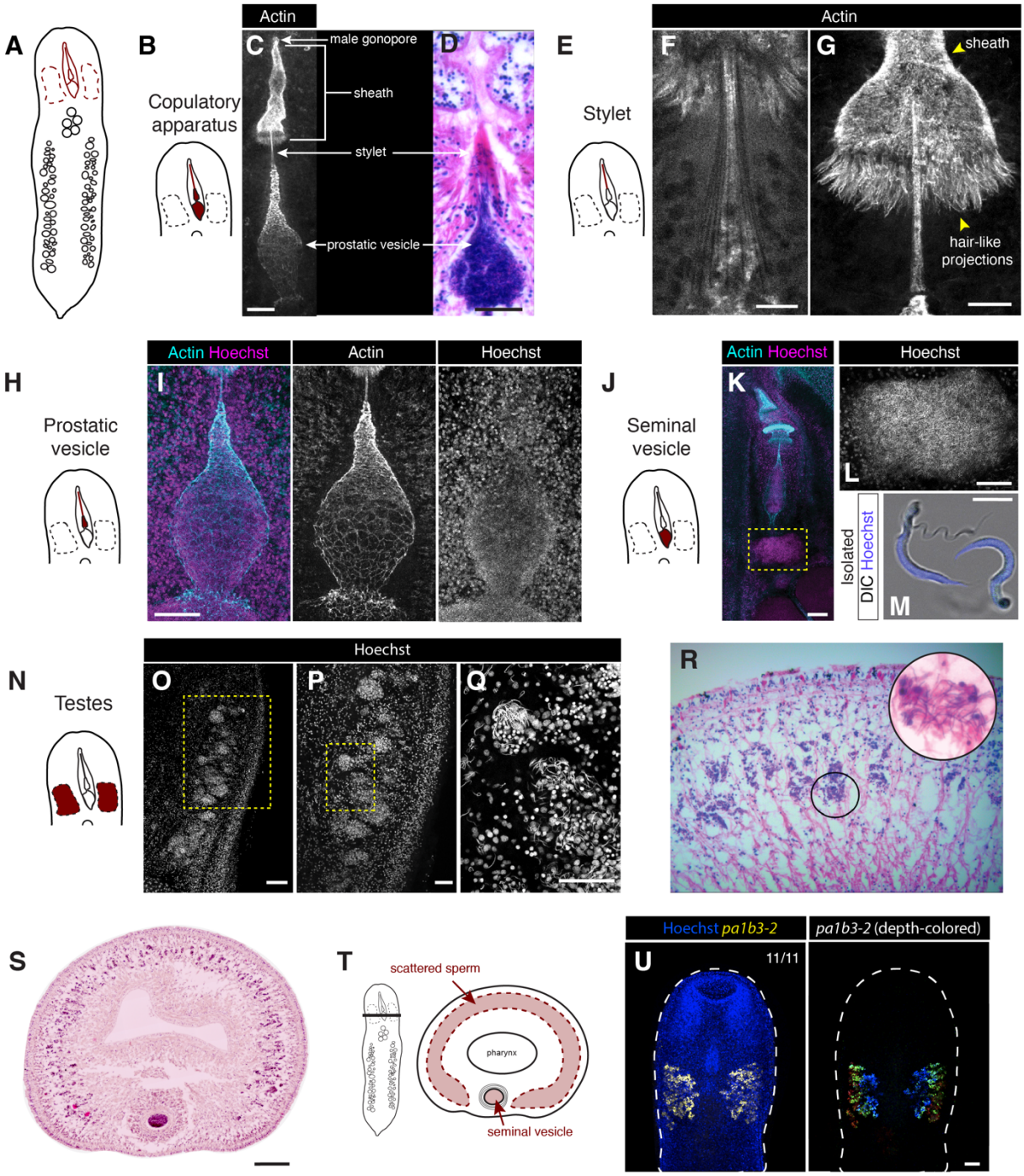

Figure 4: The male reproductive system of *Hofstenia* includes a penis with a collection of needles, a sperm containing organ (seminal vesicle), and two testes that span the dorsal surface. (**A**) A schematized view of the ventral surface of the worm with male reproductive structures highlighted in red. (**B**) Schematic of male reproductive structures with the copulatory apparatus highlighted. (**C**) Labeling with an actin dye (white) labels the male gonopore, sheath, penis stylet, and prostatic vesicle: all

374 components of the male copulatory apparatus. (**D**) A sagittal histological section also reveals these
375 organs. (**E**) Schematic of the male copulatory apparatus, with the penis stylet highlighted. (**F**) The stylet
376 includes a bundle of needles labeled by actin. (**G**) The posterior of the penis sheath terminates in a ring of
377 hair-like projections, also labeled by actin. (**H**) Schematic of the male copulatory apparatus, with the
378 prostatic vesicle highlighted. (**I**) Actin staining with a nuclear label (Hoechst) shows that the prostatic
379 vesicle is enveloped by a thin epithelium-like layer, and contains densely packed sperm. (**J**) Schematic of
380 the male copulatory apparatus, with the seminal vesicle highlighted. (**K**) The morphology of the copulatory
381 apparatus in mature, adult worms is similar to that of early adults (previous panels). (**L**) The seminal
382 vesicle of this adult worm contains densely-packed sperm. (**M**) Dissecting out an adult seminal vesicle
383 allows labeling of individual sperm cells, showing their distinctive morphology. (**N**) Schematic of the male
384 copulatory apparatus, with the testes highlighted. (**O-Q**) Nuclear staining on an adult worm, cut sagittally,
385 reveals the testes, containing dense bundles of sperm organized around clusters of cells in the
386 parenchyma. (**R-S**) Transverse histological sections confirm this organization of the testes. (**T**) Schematic
387 of a transverse view of an adult worm's anterior, showing the relative organization of the seminal vesicle
388 and testes. FISH for the male germline marker *pa1b3-2* labels much of the testes (**U**), showing that they
389 are paired organs that extend through the dorso-ventral axis of the worm (shown through depth-coloring,
390 right panel) and at least partially wrap around the head (**V**). Scale bars: 20μm (C), 10μm (F-G, M), 50μm
391 (D, I,L,P), 100μm (K,O,U), 25μm (Q), 200μm (S).
392
393
394 **The female reproductive system**
395 As observed through imaging of adult worms using a stereo microscope, the female
396 reproductive system in *H. miamia* consists of two lateral ovaries running longitudinally down
397 either side of the body, and one central cluster of mature eggs located posterior to the pharynx
398 (Fig. 5A-C). To visualize the structure of the ovaries, we used FISH to label mRNA of another
399 previously-identified germline marker: *cgnl1-2* (19). We found that this gene specifically labeled
400 the ovaries (Fig. 5D). Moreover, immunofluorescence staining with a custom antibody against

401 Piwi, a stem cell and germline marker, also labeled the ovaries (Fig. 5E). We were also able to
402 visualize the ovaries in our histological sections (Fig. 5C). These methods, together with our
403 earlier images of ovaries at different stages of development and maturity, showed that oocytes
404 were not organized by maturity within the ovary (Fig. S6A). We did not detect a membrane or
405 lining that envelopes the ovaries. This is consistent with previous work that suggests that all
406 acoels lack true ovaries *sensu stricto*: the oocytes are thought to appear and develop within the
407 parenchymal tissue without a specialized membrane or tunica to form an organ. Thus, we
408 conclude that *H. miamia*'s ovaries are asacular, in contrast to true 'sacular' gonads, which are
409 enclosed in specialized membranes (55–57).

410 Oocytes in *Hofstenia* are 'follicular'; i.e., they are surrounded by specialized cells known
411 as follicular cells (25, 55). We visualized this cell layer with immunofluorescence for Piwi and
412 histology and found that it was consistently present in every oocyte irrespective of its
413 developmental stage (Fig. 5F-G; Fig. S6B-D). We observed that many follicle cells have very
414 large nuclei, perhaps the result of the fusion of neighboring cells (Fig. 5G; Fig. S6B-C). We also
415 found clusters of sperm in the layer of follicular cells surrounding maturing oocytes of a variety
416 of developmental stages (Fig. 5F,G, insets), in agreement with Bock's (25) suggestion that the
417 follicle may 'trap' sperm and regulate the fertilization of maturing oocytes. We observed
418 significant morphological variation in the cellular components of the oocytes within the ovaries.
419 Early-stage oocytes appeared small, round or oval, although others showed irregular shapes.
420 All oocytes exhibited a granular substance primarily distributed peripherally and a large nucleus
421 - a germinal vesicle - occupying a substantial portion of the oocyte (Fig. 5H-J). The germinal
422 vesicle is arrested in prophase I of meiosis, and is found in the oocytes of nearly all animals
423 (58–61). This nucleus breaks down during early oogenesis or after fertilization (62)(63). The
424 presence of a germinal vesicle in the oocytes in *H. miamia*'s ovaries suggests that these
425 oocytes are unfertilized. It is likely that oocytes mature in the ovaries, the germinal vesicle

426 breaks down, and then oocytes are fertilized. These mature, fertilized eggs then travel from the
427 ovary to the central cavity prior to being laid.
428 We could not determine conclusively where or when fertilization happens, or where the
429 egg capsule (chorion) is produced. However, the spatial organization of the female reproductive
430 system suggests that an oocyte must mature, become fertilized, and then be transported to the
431 central cavity behind the pharynx. Across our internal examination, we did not identify any
432 oviducts, canals or additional structures that could facilitate this migration from the ovaries to the
433 central cluster. How eggs are transported thus remains unknown.
434

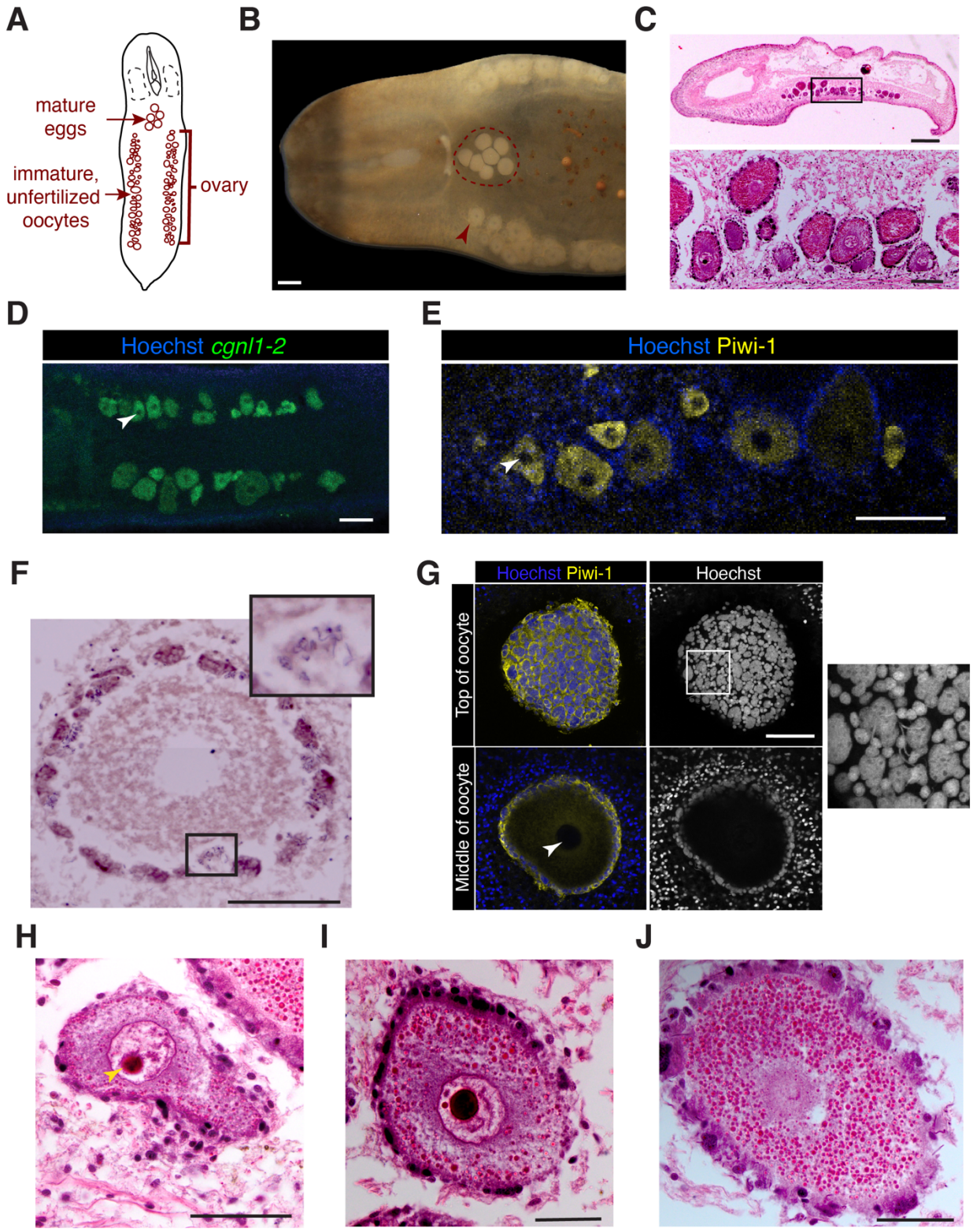

435

436 **Figure 5: The female reproductive system includes embryos stored at the base of the pharynx and**

437 **oocytes in ovaries.** (**A**) A schematized view of the ventral surface of the worm with female reproductive

438 structures highlighted. (**B**) Eggs near the pharynx of the worm (within the red circle) are fertilized and
439 mature while oocytes in ovaries (red arrow) are immature or unfertilized, with a visible germinal vesicle.
440 (**C**) A sagittal histological section reveals the organization of the follicles within an ovary. (**D**) FISH shows
441 that *cgnl1-2* labels immature oocytes (white arrow: germinal vesicle) in the ovaries. (**E**) Oocytes in ovaries
442 are also labeled by a piwi antibody (white arrow: germinal vesicle). (**F**) Histology of an ovarian follicle
443 shows that follicle cells encircle the immature oocyte. Inset: sperm cells appear to be trapped in the
444 follicle. (**G**) piwi immunofluorescence confirms the organization of the follicle (white arrow: germinal
445 vesicle)), and nuclear staining identifies trapped sperm in its surface. Histology also shows that immature
446 oocytes may have irregular shapes (**H**), contain a germinal vesicle (yellow arrow) (**H,I**), and possess an
447 abundance of (likely yolk) granules (**I,J**). Scale bars: 100μm (B, C (inset), D-F), 500μm (C), 50μm (G, H-J)
448

449 **Egg-laying behavior**

450 Egg laying has only been directly observed a few times in acoels, mostly in species belonging to
451 more recently diverged clades (13, 64) (Fig. 1B). From these observations, acoels are known to
452 lay eggs through the female gonopore (if present) (64), a mode of egg laying used by many
453 flatworms (65), or through breaks in the body wall (13, 14). It has also been suggested that
454 acoels could lay eggs through the mouth; however, attempts at direct observation of egg laying
455 have been inconclusive (13, 41).

456 Previous authors have speculated that *H. miamia* lay eggs through breaks in the body
457 wall, or perhaps partially through the mouth, but egg laying was not observed (25, 27). To
458 observe how worms lay eggs, we isolated gravid adult worms and filmed them from underneath
459 for a 24 hour period. 3 worms laid 25 eggs in these conditions. We found that worms exclusively
460 laid eggs through their mouths (Fig. 6A,B; Video 3). Egg-laying occurs in a movement lasting
461 121 ± 114 (mean ± SD) seconds, during which the worm performs a series of muscle
462 contractions to transfer a single egg from the ventral pocket of fertilized eggs into the pharynx,
463 and then further applies muscle contractions from posterior to anterior to move the egg to the
464 mouth. The worm then places each egg on the substrate with its mouth, likely secreting mucus

465 to attach the egg to the substrate (Fig. 6A,B; Video 3). Observations from these videos, as well
466 as of egg clutches in our culturing tanks, show that worms can either deposit a single egg in one
467 location or lay eggs in one or more clutches.

468 To understand the temporal dynamics of egg-laying in *H. miamia*, we then quantified the
469 time course of egg-laying in several contexts. We found that gravid worms with access to
470 mates, once isolated, continued laying eggs for over a month (Fig. 6C). It is likely that all worms
471 had recently mated given that all worms laid eggs at the onset of isolation. Juvenile worms
472 reared to adulthood in isolation also laid a single burst of eggs (Fig. 6D), multiple months after
473 first being isolated (although the timing of this burst appears to depend on rearing conditions
474 and the health of the worms). This burst of egg laying is likely the result of a selfing event in
475 which the worms fertilize their own eggs, or possibly the result of a form of parthenogenesis
476 allowing the activation of unfertilized eggs. We also allowed virgin worms to mate once, in
477 controlled conditions, and subsequently isolated them. These mated and inseminated worms
478 laid eggs for over three months after a single mating, suggesting that sperm may be stored in
479 follicular cells for several months. (Fig. 6E).

480 Finally, we asked how much control the worms had over their egg laying. Anecdotal
481 observations suggested that worms are selective about the quality of their environments, and
482 about when and where they choose to lay eggs. By quantifying the spatial positions of eggs laid
483 in their culturing tanks, we found that worms have a strong preference for laying eggs on the
484 walls of their containers, rather than on the floor (Fig. 6F). Eggs laid on walls are preferentially
485 laid close to the water line (Fig. 6G, Fig. S7A). This preference is not simply because the worms
486 lay eggs where they are: we observed that worms spend the majority of their time on the floors
487 of their boxes, and seem to rise to the surface specifically to lay eggs. These spatial
488 preferences do not seem affected by food availability: when deprived of food, egg laying still
489 primarily occurs on the walls of culture boxes (Fig. S7B). Together, this shows that worms

490 actively prefer to lay eggs close to the water line, and more generally, that substrate choice is
491 an active decision-making behavior.
492 We then asked whether worms actively choose to withhold eggs in suboptimal
493 environments. Our observations (see Fig. 3A) suggested that worms are physiologically resilient
494 to food stress, but not to reductions in water quality (data not shown). We therefore conducted
495 an experiment with a set of worms, half of which were deprived of food for one feeding period
496 (3-4 days). The other set was fed normally during this period. We found that food-deprived
497 worms laid significantly fewer eggs during this period (Fig. 6H). We hypothesized that this
498 reduction in egg-laying was because the worms were actively withholding their eggs in the
499 absence of food. Next, we repeated this experiment, first depriving some worms of food and
500 subsequently feeding them. After food-deprived worms were given food, they laid an excess of
501 eggs (Fig. 6I), suggesting that the worms actively choose to withhold egg-laying in food-limited
502 environments. More generally, these data show that *H. miamia* assess their environments to
503 make active decisions about when and where to lay eggs.
504

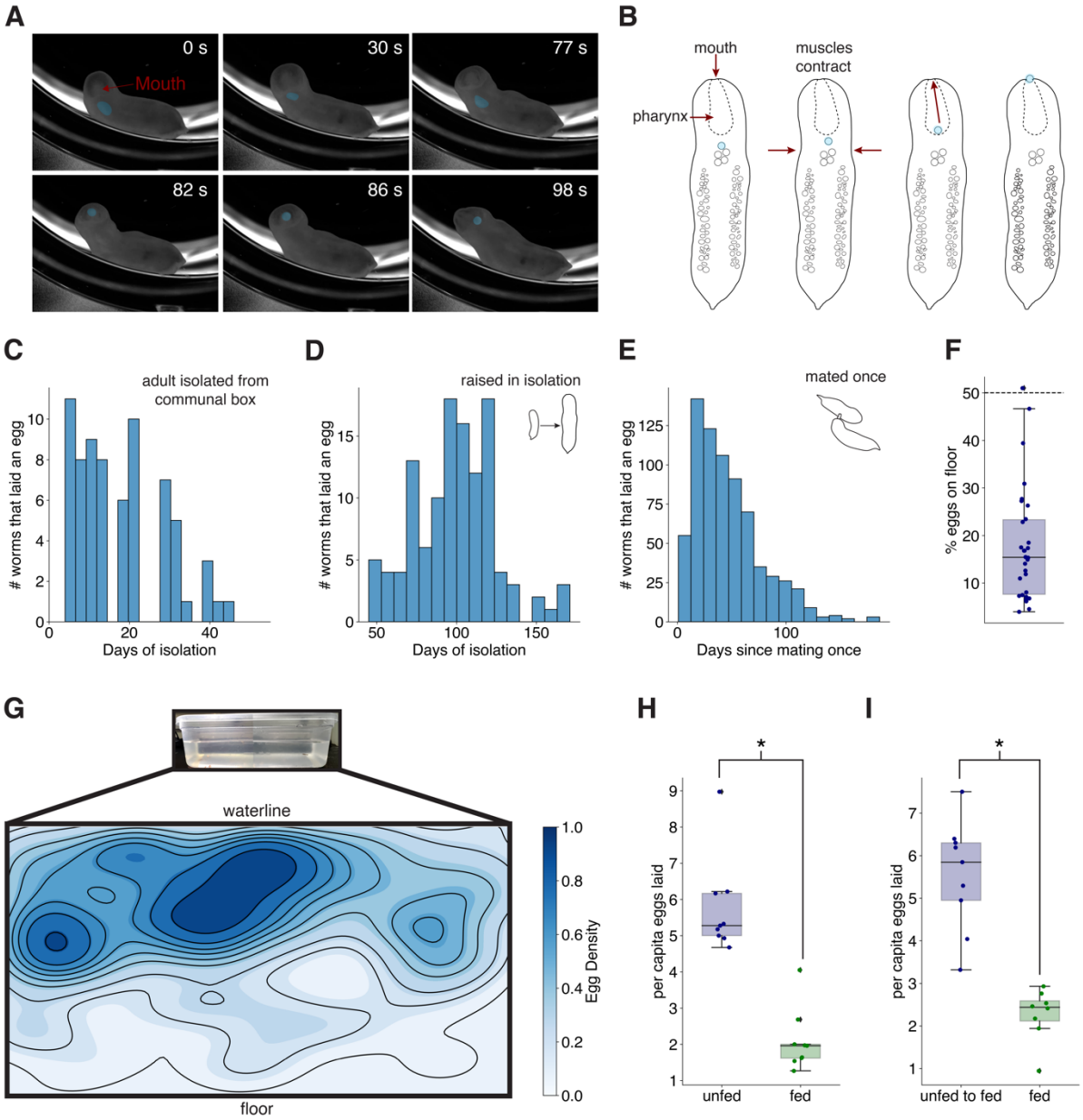

505

506 **Figure 6: *H. miamia* lays eggs through the mouth and exhibits environmental preferences in egg**
507 **laying.** (**A**) Sequence of images from a video of egg-laying. Eggs in the pharynx and emerging through
508 the mouth are shaded blue. (**B**) Schematic showing presumed process of embryo traveling from the cavity
509 beneath the pharynx to the pharynx and then out through the mouth. (**C**) Histogram showing the timing of
510 eggs laid by adult worms living in communal enclosures and then isolated. (**D**) Histogram showing the
511 timing of eggs laid by worms that undergo reproductive development in isolation and then self-fertilize. (**E**)
512 Histogram showing the timing of eggs laid by worms that are allowed to mate once. (**F**) Scatterplot of the

percentage of eggs found on the floor of communal enclosures (n = 30). This is significantly different from the expected percentage of eggs based on enclosure surface area (t-test $p < 0.0001$). (**G**) Kernel density estimate of egg locations on a subset of enclosure surfaces with similar dimensions (n = 2144 eggs). (**H**) Worms that are unfed for 4 days lay fewer eggs than fed worms (n = 9, t-test $p < 0.0001$). (**I**) Unfed worms that are then fed lay more eggs than worms that are continuously fed ($n \geq 8$, t test = < 0.0001).

Discussion

Our results provide a quantitative study of acoel reproduction for the complete life cycle from embryo to adult egg-laying at unprecedented resolution, filling a gap in our knowledge of animal reproduction in an understudied animal clade and laying a foundation for further study of anatomy, physiology, and behavior in acoels. These data have general implications for our understanding of reproductive anatomy in acoels, and for physiological and behavioral elements of reproduction.

Implications for the reproductive anatomy of acoels

Our description of *H. miamia*'s anatomy affirms many previous descriptions, including Bock's (25) observations of male and female reproductive systems of *Hofstenia atroviridis*. By using molecular techniques and high-resolution imaging we were able to expand our understanding of the functional organization of reproductive structures and to reveal aspects of *H. miamia*'s physiology. For example, in addition to locating the seminal vesicle, prostatic vesicle, and needle-like penis, we identified a ring of hair-like protrusions lining the posterior of the sheath. We speculate that during mating, muscles push the penis stylet anteriorly, through the sheath and out of the male gonopore. This movement could evert the sheath, resulting in a penis-extension state in which the sheath emerges through the gonopore around the stylet, with the ring of protrusions now near the anterior tip of the penis. It is possible that these protrusions have a sensory function, and could inform fine penis movements during hypodermic insemination. However, the behavior of the sheath has not yet been observed, and the function of the ring remains unknown.

Taxonomic implications of sperm with a single flagellum

Acoels are reported as having biflagellate sperm (6, 66), but the exact definition of "biflagellate" is unclear. This has been interpreted as the presence of two flagella (67), but it has also been

544 argued that only spermatids have two free flagella (6). Under this argument, the two flagella
545 fuse during spermatogenesis, yielding a sperm with a single flagellum that has two axonemes
546 (6, 68). This argument has been supported by ultrastructural studies of sperm, where two
547 axonemes are present in a single sperm cell (66, 69, 70) and imaging of whole sperm cells from
548 *Paratomella rubra* (69) and *Amphiscolops oni* (70), where there appears to be a single
549 flagellum. In our imaging of *H. miamia* sperm, we also observed sperm with a single flagellum.
550 The presence of a single flagellum in these three distantly related acoels supports the
551 interpretation that biflagellate refers to the presence of two axonemes rather than two free
552 flagella.
553
554 **Selfing**
555 Asexual reproduction in acoels has been demonstrated in just a handful of species that typically
556 use fission and budding to reproduce (66, 71–75). Although many other invertebrate
557 hermaphrodites, such as snails (76), tapeworms (77), and flatworms (78), are known to
558 reproduce through self-fertilization, it is thought that acoels typically reproduce through mating.
559 Our observation that *H. miamia* raised in isolation will lay eggs once reproductively mature
560 suggests that it is capable of self-fertilization (or possibly of asexual reproduction through
561 parthenogenesis). How self-fertilization could occur is unclear, but as sperm cells are observed
562 scattered through the head, it is possible they are able to migrate to the eggs in the posterior of
563 the worm. Nearly all acoels are hermaphroditic (8), and many share anatomical features with
564 *Hofstenia* (Fig. 1B). It is possible that reproduction via self-fertilization is a common life history
565 strategy across the acoels.
566
567 **Development, regeneration, and allometry**
568 Little is known about differentiation of reproductive structures in most acoels. One exception is
569 *Otocelis luteola*, an acoel that likely mates through a “genital handshake” (79) that results in

570 fertilization (45) Previous work found that the female gonopore and vagina develop first (42).
571 Sperm cells in the testes and the seminal vesicle then become visible. Roughly at the same
572 stage, oocytes also begin to develop. The ovaries later expand in size and produce increasingly
573 mature oocytes, and the vagina, female gonopore, and seminal bursa develop further. After
574 mating, the seminal bursa finally grows into its mature form. When *Otocelis luteola* is starved, it
575 experiences de-growth and de-differentiation of reproductive structures. Mature oocytes
576 disappear first, followed by sperm within the seminal vesicle. The testes are lost next, and the
577 female gonopore and other structures follow. In regenerating fragments of *Isodiametra pulchra*,
578 male structures develop and differentiate earlier than the female reproductive structures (43).
579 While sparse, these data and ours suggest that the regulation of reproductive organ growth may
580 vary across acoel species. Our data in *H. miamia* show that reproductive organs grow and scale
581 with body size, that they appear stepwise at increasing body sizes during the developmental
582 transition to adulthood, and that most of these organs are lost at the same sizes during
583 starvation-induced de-growth. Moreover, there may be size-dependent growth mechanisms that
584 ensure synchronized, symmetric organ growth. These findings enable future study of how
585 growth-relevant information is transmitted to all regions of the body to coordinate organ size
586 during growth and de-growth.
587

588 **Egg-laying dynamics and implications for life history**

589 Due to difficulties observing egg-laying, egg-laying modes are only known for a few species (13,
590 37, 41). Here, we filmed *H. miamia* laying eggs. It has been proposed that some acoels may lay
591 eggs through their mouths, a mode of egg-laying not found in other animals; here we provide
592 direct evidence that *H. miamia* do indeed lay eggs this way. We suspect that other acoels with a
593 similar suite of reproductive traits (i.e., lack of a female gonopore, a cluster of mature eggs near
594 the pharynx) could also lay eggs through their mouths. This unusual mode of egg laying raises
595 several questions. First, where in the animal does fertilization occur? Our observations suggest

596 that follicular cells surrounding immature oocytes act as a selective barrier to sperm, preventing
597 many sperm cells from reaching the oocyte, a function suggested by Bock (1923). The presence
598 of a germinal vesicle in all oocytes within the ovaries, but not in eggs in the central cavity, raises
599 the possibility that the follicle may regulate the timing of fertilization within the ovary, soon after
600 which the egg travels to the central cavity. Second, how do mature eggs travel from the lateral
601 ovaries to the central cavity, and how are the eggs in this cavity physically loaded into the
602 pharynx? Our anatomical observations have so far failed to reveal obvious oviducts, or other
603 tube-like structures that could facilitate movement of eggs into the pharynx. The only known
604 opening at the posterior of the pharynx is the pharyngeal sphincter that allows food to pass into
605 the gut. We therefore speculate that eggs travel through the gut to the central cavity, which may
606 simply be a pocket within the gut. Eggs may then be moved into the pharynx through a form of
607 reverse peristalsis (and observation of the worm prior to egg-laying shows waves of muscle
608 contraction proceeding posterior-to-anterior as each egg is loaded into the pharynx).
609 In addition to identifying the mode of egg laying in *H. miamia*, we also examined egg-
610 laying patterns over time. After a single mating, we find a peak in egg-laying around 2-3 weeks
611 later, but eggs are laid continuously for nearly 200 days. When isolated from a communal
612 enclosure where mating can happen continuously, eggs are laid for around 40 days. These
613 differences in the duration of egg laying may be in part due to corresponding differences in how
614 frequently worms mate (and in how much sperm is transferred during a single mating), and in
615 part due to cohort-specific fluctuations in water quality and other environmental factors.
616 Nonetheless, these data show that worms are able to lay eggs for months after mating,
617 suggesting that they are capable of some form of long-term sperm storage. *H. miamia* lacks an
618 anatomically-distinct organ to store sperm received during mating. We speculate that persistent
619 egg-laying following mating could be enabled by sperm trapped by the follicular cells
620 surrounding immature oocytes. As the oocytes mature, the sperm could fertilize the oocyte,
621 enabling fertilization weeks after the mating event.

Egg-laying behavior

Our results show that *H. miamia* likely makes an active choice of when and where to lay an egg once that egg is mature and fertilized. *H. miamia* has clear spatial preferences when laying an egg, preferring the area near the surface of the water. Although the worms seem to mostly be found on the floor of their enclosures, they do not prefer to lay eggs on the floor. This suggests that a worm likely navigates to a suitable position before laying an egg. This preference is robust to food deficiency. *H. miamia* also has environmental preferences, suppressing egg-laying when deprived of food and then quickly laying eggs once food is present again. Together, these results show that *H. miamia* surveys its environment and then integrates this assessment into whether - and where - it is suitable to lay an egg.

Conclusion

These findings establish a foundation of knowledge of anatomical, physiological, and behavioral elements of *H. miamia*'s reproductive life history. This enables future work on the molecular genetics of reproductive organ development and regeneration, on the physiological processes involved in egg maturation and oviposition, and on the neuroscience of reproductive behavior.

Methods

Animal husbandry

Gravid *H. miamia* are reared in communal plastic 2.25 L boxes with about 1.25 L of artificial seawater (37 ppt, pH 7.8-8.2). These communal enclosures are kept in incubators held at 21°C. Twice weekly, embryos are collected, seawater is changed, and *Artemia* sp. (brine shrimp) are

648 added. Embryos are raised in petri dishes. Once hatched, juvenile worms are raised in tanks at
649 room temperature and are fed marine rotifers *Brachionus plicatilis*. When the reproductive
650 organs begin to develop, worms are transferred to larger tanks, each typically housing 30-50
651 worms. Animals paired for mating were transferred from juvenile tanks to 24-well plates and
652 reared in isolation following similar feeding and cleaning routines as listed above. In order to
653 assay regeneration of reproductive systems, adult worms were isolated from communal
654 enclosures, anesthetized in 15% tricaine (ethyl 3-aminobenzoate methanesulfonic acid), and
655 then amputated with a dissection blade. Regenerating fragments were maintained in 6-well
656 plates and cleaned twice weekly. Five days after amputation, fragments were fed *Artemia* sp. or
657 rotifers. Animals that were starved were also maintained in 6-well plates that were cleaned twice
658 weekly but with food omitted. All animals are derived from an inbred population of worms
659 collected in 2010 from Bermuda.
660
661 **Histology**
662 Adult specimens of *H. miamia* were fixed in 4% paraformaldehyde in artificial seawater for 24
663 hours at room temperature. Following fixation, specimens were washed twice with 70% ethanol
664 to remove the fixative and then preserved in a third change of 70% ethanol for histological
665 preparation. Animals were dehydrated through a graded ethanol series (95% and 100%),
666 cleared in Histoclear, and embedded in Leica Surgipath (Paraplast) with a melting point of 56°C.
667 Longitudinal, transverse, and sagittal sections were obtained at a thickness of 5 μm using a
668 Leitz 1512 microtome. The sections were stained using a standard protocol with hematoxylin
669 and eosin and mounted on glass slides with Permount. Imaging of the sections was performed
670 using a Zeiss Axio Scan.Z1, and an Olympus BX50 microscope.
671
672 **Fluorescence in situ hybridization (FISH)**

673 Riboprobes were synthesized following protocols established in Srivastava et al. (2014).
674 Following 1-2 weeks of starvation, whole worms were fixed in 4% paraformaldehyde in artificial
675 sea water for one hour at room temperature. Fixed animals were then transferred to 24-well
676 plates in small baskets with a mesh bottom, with 4-5 animals in each basket. To remove
677 pigment autofluorescence, animals were then transferred to a bleach solution (containing 4%
678 hydrogen peroxide, SSC, and formamide) and left under a light for two hours. For all washes,
679 800 µL of solution was used. The animals were then permeabilized using proteinase K solution
680 (0.1% SDS, 1 µL/10 mL proK in PBSTx). After 10 minutes, worms were fixed again in 4%
681 formaldehyde in PBST, washed twice in PBST, and then washed in a 1:1 PBST:PreHyb solution
682 for 10 minutes. Specimens were then incubated in the PreHyb solution (50% DI formamide,
683 25% 20X SSC, 0.05% 10% Tween-20, 1mg/mL yeast tRNA, 20% water) for two hours in a 56°C
684 hybridization oven and then transferred to a hybridization solution (50% DI formamide, 25% 20X
685 SSC, 0.05% 10% Tween-20, 1 mg/mL yeast tRNA, 10% 50% dextran sulfate, 10% water)
686 containing riboprobe(s) and left overnight. The specimens were then put through several 30-
687 minute washes at 56°C, starting with two PreHyb washes, two 1:1 PreHyb:2XSSCT washes,
688 two 2XSSCT (2XSSC with 0.1% TritonX-100) solution washes, two 0.2XSSCT (0.2X SSC with
689 0.1% TritonX-100) solution washes. Specimens were then left to cool at room temperature and
690 then washed in two ten-minute PBST washes. A 1-hour blocking at room temperature was then
691 performed with blocking solution (5% horse serum and 5% casein in PBST). Animals were then
692 incubated with anti-Digoxigenin-POD (1:1500 dilution; Roche, 11633716001) in a blocking
693 buffer overnight. The following day, animals were washed 6 times with PBST, incubated with a
694 tyramide buffer (1.1688g/mL NaCl, 6.18mg/mL boric acid, filled with water and adjusted pH to
695 8.5) for 10 minutes, then developed with rhodamine-conjugated tyramide solution for 10
696 minutes. Animals were washed again with PBST and incubated for 1 hour in 1:500
697 PBST:Hoechst to label nuclei. Animals were then mounted on glass slides with
698 VECTASHIELD® PLUS Antifade Mounting Medium (Vector Laboratories, H-1900).

699

700 **Whole-mount immunofluorescence**

701 Worms were fixed in 4% paraformaldehyde (Electron Microscopy Sciences, 15714) in artificial
702 sea water for 1-2 hours at room temperature (juveniles were fixed for one hour, adults were
703 fixed for two) before washing with PBST (PBS + 0.1% Triton-X-100). Adult worms were
704 anesthetized in 15% tricaine for 5 minutes prior to fixation to minimize epidermal rupture. For
705 immunofluorescence, worms were washed in PBST, blocked for one hour at room temperature
706 in 10% goat serum in PBST, and incubated in primary antibody for 48-72 hours at 4C on a
707 shaker (juveniles only require 48 hours, adults need the full 72 hours). The following day, worms
708 were washed thoroughly in PBST (8 x 20 min washes) on a nutator before blocking for one hour
709 at room temperature on a shaker. Worms were incubated in secondary antibody overnight at
710 4C; the following day, worms were washed thoroughly in PBST (8 x 20 in washes) on a shaker
711 before adding direct conjugate dyes and mounting on glass slides with VECTASHIELD®
712 HardSet™ Antifade Mounting Medium (Vector Laboratories, H-1400-10). Antibodies used:
713 Tropomyosin (custom, (80), Piwi-1 (custom), Par3 (St. John's Laboratory, STJ502116), Goat
714 anti-Rabbit IgG (H+L) Cross-Adsorbed Secondary Antibody, Alexa Fluor™ 568 (ThermoFisher,
715 A-11011), Hoechst (ThermoFisher, H1399), SiR-actin (Cytoskeleton, CY-SC001). All images
716 with FISH and immunofluorescence were acquired with a Leica SP8 point-scanning confocal
717 microscope.

718

719

720 **Quantitative analysis of development, regeneration, and de-growth**

721 We collected 42 zygotes laid from wild-type worms. Each embryo was transferred to a well of a
722 24-well cell culture plate with artificial seawater. Plates were stored in a temperature-controlled
723 incubator. Without removing the embryos from the plate, they were imaged twice weekly
724 through a dissection microscope with white illumination from LEDs mounted above the sample.

725 Water was also changed on these days. The same volume of water was added to each well
726 (2.35 mL in each 12-well). Once at least one embryo had hatched, rotifers were added to each
727 well. On each feeding day, the concentration of rotifers was calculated by counting the number
728 of rotifers in diluted samples. Based on this concentration, the volume of rotifers was altered to
729 ensure a consistent number of rotifers was given to each animal. At different stages during the
730 experiment, the number of rotifers (Fig. S2A) fed increased. Increases were gradual to ensure
731 worms always had more food than they could eat, while minimizing excess food which could
732 affect water quality. Hatched worms were removed from wells for imaging twice weekly. Worms
733 were anesthetized in tricaine (15% ethyl 3-aminobenzoate, methanesulfonic acid salt; Sigma-
734 Aldrich #E10521), and mounted on microscope slides with a 20x20 mm sticker grid with 1mm
735 resolution (ThomasScientific, #1207X53). When worms were larger, they were moved to larger
736 6-well plates in 10 mL of artificial sea water and began to be fed brine shrimp as well (Fig.
737 S2A). The number of brine shrimp added was measured using the same concentration
738 procedure outlined above for rotifers. Once worms had matured, the number of brine shrimp
739 increased.

740 Images were manually annotated in FIJI. A line was drawn to capture the length of the
741 sticker grid to define an image-specific scale. Additional lines were drawn to measure the length
742 from the most posterior part of the male reproductive system (e.g., base of the penis tube before
743 sperm production begins or base of the seminal vesicle) to the male gonopore, the length of the
744 seminal vesicle, the length of each ovary, the length of the worm's body, and the width of the
745 worm's body. Measurements were converted to mm using image-specific scale information.
746 Penis length was calculated by subtracting the length of the seminal vesicle from the length of
747 the male gonad.

748 These imaging and measurement processing procedures were repeated with starving
749 worms and regenerating worm fragments. Starved and fed control worms were anesthetized
750 and imaged roughly once a week for 11 weeks. 106 days after isolation, starved worms were

751 imaged again, at which point one starved worm had died. Regenerating worms were imaged
752 starting 2 days post-amputation and then every 2-5 days until 25 days post-amputation at which
753 point images were taken less frequently. Regenerating fragments were not fed for the first four
754 days after amputation, and were then fed normally. In these experiments, a two-pointed line or
755 multi-jointed spline was used to measure lengths. All analyses were then performed in python,
756 with code assistance from GPT4.
757
758 **Egg-laying behavior**
759 Adult worms from a communal tank were moved to individual wells in the center of a 24-well
760 plate or 12-well plate (Fisher Scientific #07-200-82). We mounted the plate on an elevated
761 platform within an enclosed behavioral rig. The plate was illuminated with uniform white light,
762 from addressable LEDs (Adafruit #SK6812RGBW, powered by 5V DC) arranged in a ring
763 around the plate behind a white acrylic diffuser (McMaster-Carr #8505K741). An infrared
764 camera (Basler Ace ac4024-29um USB 3.0 monochrome) was mounted underneath the plate to
765 allow filming of the worm's ventral surface. A USB fan (Amazon #B0C27NGKCV) was mounted
766 on the floor of the behavioral chamber for temperature regulation. We filmed worms at 1Hz for
767 8-12 hours. After filming, each worm was returned to its original communal tank.
768 To find egg positions, communal tanks were maintained according to our husbandry
769 protocol. Every 3-4 days, before cleaning, images were taken of each face of the box (2 short
770 faces, 2 long faces, and the floor of the box). The x- and y-coordinates of the eggs in small and
771 long face images were scored in FIJI. The positions of eggs laid on the floor were not scored
772 due to low density. The x- and y-coordinates of the boundaries of the water in each image were
773 also scored. From these image-specific boundaries, a common set of bounds was calculated for
774 each type of face (i.e., short, long). Egg coordinate positions were then scaled and aligned to
775 these common bounds for analysis.

For experiments measuring when worms laid eggs, communal enclosures of adult worms were cleaned twice weekly and fed well. Three days later, eggs were collected from each box and counted. On this day, half of these enclosures were randomly selected to have food withheld. After four days with or without food, eggs were collected from all boxes and counted. To test whether egg laying is recovered when unfed worms are fed, communal enclosures of adult worms were randomly selected to have food or to have food withheld. Four days later, eggs were collected and counted and then all communal enclosures were fed. Three days later, eggs were collected and counted.

Author Contributions

VC, SET, and MS designed the project; SET and VC performed development, physiology and behavior experiments; VC and SET analyzed the data; APK performed and interpreted immunofluorescence and imaging experiments; DMB performed and interpreted histology experiments in the context of prior anatomical literature; VC, SET, and MS wrote the manuscript with input from all authors; and MS supervised the project.

Acknowledgements

We thank Gonzalo Giribet, Matthew Hooge, James Hanken, Javier Ortega-Hernandez, Andrew Berry, and all members of the Srivastava lab for helpful discussion. We also thank James Hanken, Júlia Chaumel, and Christina Daly for histology help and infrastructure. VC and APK are Fellows of the Jane Coffin Childs Fund for Medical Research. ST acknowledges funding from the Harvard Museum of Comparative Zoology, Herchel Smith Undergraduate Science Research Program, and the Program for Research in Science and Engineering. This project was supported by grants from the National Institute of General Medical Sciences of the NIH to MS: R35GM128817 and R35GM153252.

References

1. N. Davies, J. Krebs, S. West, *An Introduction to Behavioural Ecology* (Wiley-Blackwell, 2013).

2. J. T. Cannon, *et al.*, Xenacoelomorpha is the sister group to Nephrozoa. *Nature* **530**, 89–93 (2016).

3. P. Kapli, M. J. Telford, Topology-dependent asymmetry in systematic errors affects phylogenetic placement of Ctenophora and Xenacoelomorpha. *Sci Adv* **6**, eabc5162 (2020).

4. H. Philippe, *et al.*, Acoelomorph flatworms are deuterostomes related to Xenoturbella. *Nature* **470**, 255–258 (2011).

5. Tyler, S., Schilling, S., Hooge, M., & Bush, L. F., Turbellarian taxonomic database. Version 1.7. (2012). Available at: http://turbellaria.umaine.edu.

6. J. G. Achatz, M. Chiodin, W. Salvenmoser, S. Tyler, P. Martinez, The Acoela: on their kind and kinships, especially with nemertodermatids and xenoturbellids (Bilateria incertae sedis). *Org. Divers. Evol.* **13**, 267–286 (2013).

7. A. Wallberg, The Stylet - Diversity and Systematics of Acoela and Nemertodermatida. (2012). Available at: http://acoela.myspecies.info.

8. U. Jondelius, A. Wallberg, M. Hooge, O. I. Raikova, How the Worm Got its Pharynx: Phylogeny, Classification and Bayesian Assessment of Character Evolution in Acoela. *Syst. Biol.* **60**, 845–871 (2011).

9. Y. V. Mamkaev, Etude morphologique d'*Actinoposthia beklemischevi* n. sp. (Turbellaria

824 Acoela). *Cah. Biol. Mar.* **6**, 23–50 (1965).

825 10. O. Raikova, A. Falleni, V. Gremigni, Oogenesis in *Actinoposthia beklemischevi*
826 (Platyhelminthes, Acoela): an ultrastructural and cytochemical study. *Tissue Cell* **27**, 621–
827 633 (1995).

828 11. G. Giribet, G. D. Edgecombe, *The Invertebrate Tree of Life* (Princeton University Press,
829 2020).

830 12. X. Bailly, *et al.*, The chimerical and multifaceted marine acoel *Symsagittifera roscoffensis*:
831 from photosymbiosis to brain regeneration. *Front. Microbiol.* **5**:498 (2014).

832 13. H. M. Costello, D. P. Costello, Egg laying in the acoelous turbellarian *Polychoerus*
833 *carmelensis*. *Biol. Bull.* **76**, 80–89 (1939).

834 14. G. Apelt, Fortpflanzungsbiologie, Entwicklungszyklen und vergleichende Frühentwicklung
835 acoeler Turbellarien. *Mar. Biol.* **4**, 267–325 (1969).

836 15. T. Shannon, J. Achatz, *Convolutriloba macropyga* sp. nov., an uncommonly fecund acoel
837 (Acoelomorpha) discovered in tropical aquaria. *Zootaxa* **1525**, 1–17 (2007).

838 16. T. Zauchner, W. Salvenmoser, B. Egger, A cultivable acoel species from the
839 Mediterranean, *Aphanostoma pisae* sp. nov. (Acoela, Acoelomorpha). *Zootaxa* **3941**, 401–
840 413 (2015).

841 17. K. De Mulder, *et al.*, Characterization of the stem cell system of the acoel *Isodiametra*
842 *pulchra*. *BMC Dev. Biol.* **9**, 69 (2009).

843 18. M. Srivastava, Studying development, regeneration, stem cells, and more in the acoel
844 *Hofstenia miamia*. *Curr. Top. Dev. Biol.* **147**, 153–172 (2022).

19. R. E. Hulett, *et al.*, Acoel single-cell atlas reveals expression dynamics and heterogeneity of adult pluripotent stem cells. *Nat. Commun.* **14**, 2612 (2023).

20. L. Ricci, M. Srivastava, Transgenesis in the acoel worm *Hofstenia miamia*. *Dev. Cell* **56**, 3160–3170.e4 (2021).

21. J. O. Kimura, D. M. Bolaños, L. Ricci, M. Srivastava, Embryonic origins of adult pluripotent stem cells. *Cell* **185**, 4756–4769.e13 (2022).

22. A. R. Gehrke, *et al.*, Acoel genome reveals the regulatory landscape of whole-body regeneration. *Science* **363**: eaau6173 (2019).

23. J. O. Kimura, L. Ricci, M. Srivastava, Embryonic development in the acoel *Hofstenia miamia*. *Development* **148**, dev188656 (2021).

24. M. Hooge, *et al.*, A revision of the systematics of panther worms (*Hofstenia* spp., Acoela), with notes on color variation and genetic variation within the genus. *Hydrobiologia* **592**, 439–454 (2007).

25. S. Bock, *Eine neue marine Turbellariengattung aus Japan* (Almqvist & Wiksell, 1923).

26. D. D. Corrêa, Two New Marine Turbellaria from Florida. *Bull. Mar. Sci.* **10**, 208–216 (1960).

27. O. Steinböck, Grundsätzliches zur Evolution der Turbellarien. *Zeitschrift für Zoologische Systematik und Evolutionsforschung* **4**, 58–195 (1966).

28. S. Beltagi, A. Mandura, *Hofstenia arabiensis* Nov. Sp. (Hofsteniidae): A New Species of Acoelan Turbellaria from the Red Sea North of Jeddah. *Journal of King Abdulaziz University-science* **3**, 65–90 (1991).

29. A. Faubel, B. Cameron, Platyhelminthes from salt marshes of Coomera River,

Southeastern Queensland, Australia. *Mem Queensland Mus* **46**, 511–519 (2001).

30. J. Dörjes, Die Acoela (Turbellaria) der Deutschen Nordseeküste und ein neues System der Ordnung. *J. Zoolog. Syst. Evol. Res.* **6**, 56–452 (1968).

31. M. Boone, W. Houthoofd, W. Bert, T. Artois, First record of Nemertodermatida from Belgian marine waters. *Belg. J. Zool.* **141**, 62–64 (2011).

32. W. E. Sterrer, New and known Nemertodermatida (Platyhelminthes- Acoelomorpha) - a revision. *Belgian Journal of Zoology* **128**, 55–92 (1998).

33. J. G. Achatz, M. D. Hooge, Convolutidae (Acoela) from Tanzania. *Zootaxa* **1362**, 1 (2006).

34. M. Hooge, Two new families, three new genera, and five new species of acoels (Acoela Platyhelminthes) from Queensland Australia. *Cah. Biol. Mar.* **44**, 275–298 (2003).

35. M. Hooge, J. P. S. Smith, New acoels (Acoela, Acoelomorpha) from North Carolina. *Zootaxa* **442**, 1–24 (2004).

36. H. M. Costello, D. P. Costello, Copulation in the acoelous turbellarian *Polychoerus carmelensis*. *Biol. Bull.* **75**, 85–98 (1938).

37. E. Gardiner, Early development of *Polychoerus caudatus*, Mark. *J. Morphol.* **11**, 155–176 (1895).

38. L. H. Hyman, Reproductive system and copulation in *Amphiscolops langerhansi* (Turbellaria Acoela). *Biol. Bull.* **72**, 319–326 (1937).

39. F. Peebles, A Description of three Acoela from the Gulf of Naples. *Mitteilungen a.d. Zool. Station zu Neapel* **22**, 292–312 (1915).

40. L. Bush, Biology of *Neochilda fusca* N. gen., n. sp. from the northeastern coast of the

887 United States (Platyhelminthes: Turbellaria). *Biol. Bull.* **148**, 35–48 (1975).

888 41. M. C. Watzin, Egg laying in the acoel turbellarian *Neochildia fusca*. *Trans. Am. Microsc.*
889 *Soc.* **103**, 322–325 (1984).

890 42. E. N. Kozloff, A new genus and five new species of acoel flatworms from the Pacific coast
891 of North America, and resolution of some systematic problems in the families Convolutidae
892 and Otocelididae. *Cah. Biol. Mar.* **41**, 281–293 (2000).

893 43. E. Perea-Atienza, *et al.*, Posterior regeneration in *Isodiametra pulchra* (Acoela,
894 Acoelomorpha). *Front. Zool.* **10**, 64 (2013).

895 44. N. W. Riser, *Nemertinoides elongatus* gen. n., sp. n. (Turbellaria: Nemertodermatida) from
896 coarse sand beaches of the Western North Atlantic. *Proc. Helminthol. Soc. Wash.* **54**, 60–
897 67 (1987).

898 45. D. Grae, E. Kozloff, Post-copulatory storage of sperm in the seminal bursa of the acoel
899 flatworm *Otocelis luteola*. *Invertebr. Reprod. Dev.* **35**, 151–154 (1999).

900 46. I. Meyer-Wachsmuth, M. Curini Galletti, U. Jondelius, Hyper-cryptic marine meiofauna:
901 species complexes in Nemertodermatida. *PLoS One* **9**, e107688 (2014).

902 47. M. Crezee, *Paratomella rubra* Rieger and Ott, an amphiatlantic acoel turbellarian. *Cah. Biol.*
903 *Mar.* **19**, 1–9 (1978).

904 48. A. G. Kostenko, The position of Taurida fulvomaculata (Ax, 1959) in the system of Acoela.
905 In: Morphology of turbellarians. *Akad Nauk USSR Trudy Zool* **195**, 14–25 (1989).

906 49. J. Dörjes, *Paratomella unichaeta*, nov. gen. nov. spec., Vertreter einen neuen Familie der
907 Turbellaria Acoela mit asexueller Fortpflanzung durch Paratomie. *Veröffentlichungen des*
908 *Instituts für Meeresforschung in Bremerhaven* **II**, 187–200 (1966).

50. A. Faubel, Die Acoela (Turbellaria) eines Sandstrandes der Nordseeinsel Sylt. *Mikrofauna Meeresbodens* **32**, 1–58 (1974).

51. A. Faubel, Interstitielle Acoela (Turbellaria) aus dem Littoral der nordfriesischen Inseln Sylt und Amrum. *Mitt. Hamb. Zool. Mus. Inst.* **73**, 17–56 (1976).

52. M. Srivastava, K. L. Mazza-Curll, J. C. van Wolfswinkel, P. W. Reddien, Whole-Body Acoel Regeneration Is Controlled by Wnt and Bmp-Admp Signaling. *Curr. Biol.* **24**, 1107–1113 (2014).

53. L. H. Hyman, *The invertebrates: Platyhelminthes and Rhynchocoela. The acoelomate Bilateria* (McGraw-Hill, New York, 1951).

54. A. Faubel, The Polycladida, Turbellaria. Proposal and establishment of a new system. Part I. The Acotylea. *Mitt. Hamb. Zool. Mus. Inst.* **80**, 17–121 (1983).

55. R. M. Rieger, S. Tyler, J. P. S. Smith, G. E. Rieger, “Platyhelminthes and Nemertinea” in *Microscopic Anatomy of Invertebrates*, (Wiley-Liss, 1991), pp. 7–140.

56. A. Schmidt-Rhaesa, *The Evolution of Organ Systems* (OUP Oxford, 2007).

57. K. Eckelbarger, A. Hodgson, Invertebrate oogenesis – a review and synthesis: comparative ovarian morphology, accessory cell function and the origins of yolk precursors. *Invertebr. Reprod. Dev.* **65**, 71–140 (2021).

58. C. Munro, H. Cadis, S. Pagnotta, E. Houliston, J.-R. Huynh, Conserved meiotic mechanisms in the cnidarian *Clytia hemisphaerica* revealed by *Spo11* knockout. *Sci Adv* **9**, eadd2873 (2023).

59. J.-L. Liu, M. Buszczak, J. G. Gall, Nuclear bodies in the *Drosophila* germinal vesicle. *Chromosome Res.* **14**, 465–475 (2006).

931 60. H. Grossman, *et al.*, Regulation of GVBD in mouse oocytes by miR-125a-3p and Fyn
932 kinase through modulation of actin filaments. *Sci. Rep.* **7**, 2238 (2017).

933 61. L. Herlands, G. G. Maul, Characterization of a major nucleoplasmin-like germinal vesicle
934 protein which is rapidly phosphorylated before germinal vesicle breakdown in *Spisula*
935 *solidissima*. *Dev. Biol.* **161**, 530–537 (1994).

936 62. N. Sagata, Meiotic metaphase arrest in animal oocytes: its mechanisms and biological
937 significance. *Trends Cell Biol.* **6**, 22–28 (1996).

938 63. A. Falleni, V. Gremigni, Ultrastructural study of oogenesis in the acoel turbellarian
939 Convoluta. *Tissue Cell* **22**, 301–310 (1990).

940 64. E. Gardiner, *The Growth of the Ovum, Formation of the Polar Bodies, and the Fertilization*
941 *in Polychaerus Caudatus* (1898).

942 65. S. J. W. Tong, R. S. L. Ong, Mating behavior, spawning, parental care, and embryonic
943 development of some marine pseudocerotid flatworms (Platyhelminthes: Rhabditophora:
944 Polycladida) in Singapore. *Invertebr. Biol.* **139**, e12293 (2020).

945 66. Y. I. Zabotin, V. G. Evtugyn, Ultrastructure of spermatozoa and female copulatory organs in
946 preferably asexually-reproducing acoel *Convolutriloba retrogemma* (Acoelomorpha).
947 *Zoomorphology* **140**, 19–26 (2021).

948 67. S. J. Bourlat, A. Hejnol, Acoels. *Curr. Biol.* **19**, R279–280 (2009).

949 68. A. Petrov, M. Hooge, S. Tyler, Ultrastructure of sperms in Acoela (Acoelomorpha) and its
950 concordance with molecular systematics. *Invertebr. Biol.* **123**, 183–197 (2004).

951 69. O. I. Raikova, A. Falleni, J.-L. Justine, Spermiogenesis in *Paratomella*
952 *rubra*(Platyhelminthes, Acoela): Ultrastructural, immunocytochemical, cytochemical studies

and phylogenetic implications. *Acta Zool.* **78**, 295–307 (1997).

70. M. Asai, H. Miyazawa, R. Yanase, K. Inaba, H. Nakano, A new species of Acoela possessing a middorsal appendage with a possible sensory function. *Zoolog. Sci.* **39**, 147–156 (2022).

71. B. Åkesson, *et al.*, Fission in *Convolutriloba longifissura*: asexual reproduction in acoelous turbellarians revisited. *Acta Zool.* **82**, 231–239 (2001).

72. P. Ax, E. Schulz, Ungeschlechtliche Fortpflanzung durch Paratomie bei acoelen Turbellarien. *Biol. Zent. Bl.* **78**, 613–622 (1959).

73. E. du Bois-Reymond Marcus, On Turbellaria and Polygordius from the Brazilian Coast. *Bol Fac Fil Ci Letr Univ Sao Paulo Zool* **20**, 19–53 (1955).

74. E. D. Hanson, Asexual reproduction in Acoelous Turbellaria. *Yale J. Biol. Med.* **33**, 107–111 (1960).

75. K. Ishikawa, T. Yamasu, An acoel flat worm species related closely to the species *Convolutriloba retrogemma* Hendelberg and Akesson occurs in Okinawa Island, Ryukyu Archipelago. *Zoological Science* **9**, 1281 (1992).

76. P.-Y. Henry, L. Vimond, T. Lenormand, P. Jarne, Is delayed selfing adjusted to chemical cues of density in the freshwater snail *Physa acuta*? *Oikos* **112**, 448–455 (2006).

77. M. Milinski, Fitness consequences of selfing and outcrossing in the cestode Schistocephalus solidus. *Integr. Comp. Biol.* **46**, 373–380 (2006).

78. A. Giannakara, S. A. Ramm, Self-fertilization, sex allocation and spermatogenesis kinetics in the hypodermically inseminating flatworm *Macrostomum pusillum*. *J. Exp. Biol.* **220**, 1568–1577 (2017).

79. N. K. Michiels, L. J. Newman, Sex and violence in hermaphrodites. *Nature* **391**, 647–647 (1998).

80. R. E. Hulett, D. Potter, M. Srivastava, Neural architecture and regeneration in the acoel *Hofstenia miamia*. *Proceedings of the Royal Society B: Biological Sciences* **287**, 20201198 (2020).